An Explicit Characterization of Minimum Wheel-Rotation Paths for Differential-Drives

Hamidreza Chitsaz, Steven M. LaValle, Devin J. Balkcom, and Matthew T. Mason

***Abstract*— This paper characterizes shortest paths for differential-drive mobile robots by classifying solutions in the spirit of Dubins curves and Reeds-Shepp curves for car-like robots. Not only are optimal paths for mobile robots interesting with respect to the optimized criteria, but also they offer a family of motion primitives that can be used for motion planning in the presence of obstacles. A well-defined notion of *shortest* is obtained by optimizing the total amount of wheel rotation. This paper extends our previous characterization of the minimum wheel-rotation trajectories that are maximal with respect to sub-path partial order in [2]. To determine the shortest path for every pair of initial and goal configurations, we need to characterize all of the minimum wheel-rotation trajectories regardless of whether they are maximal with respect to sub-path partial order. In this paper we give all 52 minimum wheel-rotation trajectories. We also give the end-point map in terms of the path parameters for every shortest path. Thus, finding the shortest path for every pair of initial and goal configurations reduces to solving systems of equations for the path parameters. As in [2], the Pontryagin Maximum Principle as a necessary condition eliminates some non-optimal paths. The paths that satisfy the Pontryagin Maximum Principle (called extremals) are presented in this paper by finite state machines. Level sets of the cost-to-go function for a number of robot orientations are finally presented.**

I. Introduction

This paper presents the complete family of all 52 minimum wheel-rotation trajectories for differential-drive mobile robots in the plane without obstacles. By *wheel-rotation* we mean the distance travelled by the robot wheels, which is independent of the robot maximum speed. Thus, minimizing wheel-rotation is a natural variation of the shortest path problem by Dubins [4] and Reeds and Shepp [6], in which the distance travelled by the car is minimized. In this regard, this work has been basically motivated by Dubins and Reeds-Shepp shortest paths for car-like vehicles. In fact, we show that some Reeds-Shepp curves appear in the set of minimum wheel-rotation trajectories, whereas there are minimum wheel-rotation trajectories that are different from Reeds-Shepp curves.

The first work on shortest paths for car-like vehicles is done by Dubins [4]. He gives a characterization of time-optimal trajectories for a car with a bounded turn radius. In that problem, the car always moves forward with constant speed. He uses a purely geometrical method to characterize such shortest paths. Later, Reeds and Shepp [6] solve a similar problem in which the car is able to move backward as well. They identify 48 different shortest paths. Shortly after Reeds and Shepp, their problem is solved and also refined by Sussmann and Tang [11] with the help of optimal control techniques. Sussmann and Tang show that there are only 46 different shortest paths for Reeds-Shepp car. Souères and Laumond [9] classify the shortest paths for a Reeds-Shepp car into symmetric classes.

However, optimal trajectories for nonholonomic systems are interesting not only because of the criterion that they optimize, but also because they have a property that makes them useful for motion planning in the presence of obstacles. If we restrict the motions of the system to the set of optimal trajectories, we still conserve some important properties of the system such as *small-time local controllability*. Consequently, local planners that are based on families of optimal trajectories satisfy the *topological property* [7]. Hence, different families of optimal trajectories provide local planners that can be helpful in different applications.

In [1], the time-optimal trajectories for the differential drive is studied, and a complete characterization of all time-optimal trajectories is given. Time-optimal trajectories for the differential drive consist of rotation in place and straight line segments. Minimum wheel-rotation trajectories are composed of rotation in place, straight line, and swing segments (one wheel stationary and the other rolling). In this paper we extend our previous characterization of the minimum wheel-rotation trajectories, which are maximal with respect to sub-path partial order, to derive all 52 different minimum wheel-rotation trajectories.

Souères and Boissonnat [8] study the time optimality of Dubins car with angular acceleration control. They present an incomplete characterization of time-optimal trajectories for their system. However, full characterization of such time-optimal trajectories seems to be difficult because Sussmann [10] proves that there are time-optimal trajectories for that system that require infinitely many input switchings (chattering or Fuller phenomenon). Sussmann uses Zelikin and Borisov theory of chattering control [12] to prove his result. Chyba and Sekhavat [3] study time optimality for a mobile robot pulling one trailer.

We first present finite state machines for extremals. We then give an explicit characterization of all 52 minimum wheel-rotation paths with their end-point map in terms of the path parameters. Finally, we give level sets of the cost-to-go function computed at a number of robot orientations. The proofs of lemmas are omitted due to space limitations.

H. Chitsaz and S.M. LaValle are with Department of Computer Science, University of Illinois at Urbana-Champaign, {chitsaz, lavalle}@cs.uiuc.edu.

D.J. Balkcom is with Department of Computer Science, Dartmouth College, devin.balkcom@dartmouth.edu.

M.T. Mason is with Robotics Institute, Carnegie Mellon University, matt.mason@cs.cmu.edu.

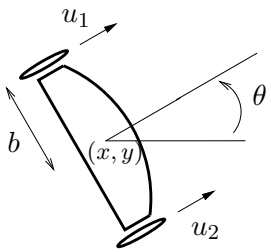

Fig. 1. Differential-drive model

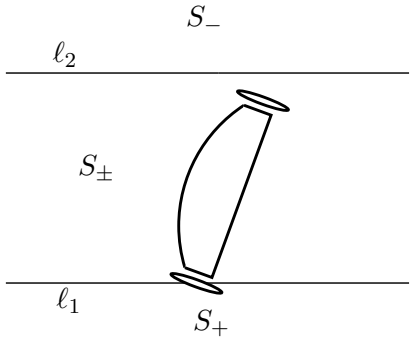

Fig. 2. Robot stays between two lines ℓ_1 and ℓ_2 along a tight extremal.

II. Problem Formulation

A differential-drive robot [2] is a three-dimensional system with its configuration variable denoted by $q = (x, y, \theta) \in \mathcal{C} = \mathbb{R}^2 \times \mathbb{S}^1$ in which x and y are the coordinates of the point on the axle, equidistant from the wheels, in a fixed frame in the plane, and $\theta \in [0, 2\pi)$ is the angle between x-axis of the frame and the robot local longitudinal axis (see Figure 1).

The robot has independent velocity control of each wheel. Assume that the wheels have equal bounds on their velocity. More precisely, $u_1, u_2 \in [-1, 1]$, in which the inputs u_1 and u_2 are respectively the left and the right wheel velocities, and the input space is $U = [-1, 1] \times [-1, 1] \subset \mathbb{R}^2$. The system is

$$\dot{q} = f(q, u) = u_1 f_1(q) + u_2 f_2(q) \tag{1}$$

in which f_1 and f_2 are vector fields in the tangent bundle $T\mathcal{C}$ of configuration space. Let the distance between the robot wheels be $2b$. In that case,

$$f_1 = \frac{1}{2}\begin{pmatrix}\cos\theta\\ \sin\theta\\ -\frac{1}{b}\end{pmatrix} \text{ and } f_2 = \frac{1}{2}\begin{pmatrix}\cos\theta\\ \sin\theta\\ \frac{1}{b}\end{pmatrix}. \tag{2}$$

The Lagrangian L and the cost functional J to be minimized are

$$L(u) = \frac{1}{2}(|u_1| + |u_2|) \tag{3}$$

$$J(u) = \int_0^T L(u(t))dt. \tag{4}$$

The factor $\frac{1}{2}$ above helps to simplify further formulas, and does not alter the optimal trajectories.

For every pair of initial and goal configurations, we seek an admissible control, i.e. a measurable function $u\colon [0, T] \to U$, that minimizes J while transferring the initial configuration to the goal configuration. Since the cost J is invariant by scaling the input within U, we can assume without loss of generality that the controls are either constantly zero ($u \equiv (0, 0)$) or saturated at least in one input, i.e. $\max(|u_1(t)|, |u_2(t)|) = 1$ for all $t \in [0, T]$. Note that throughout this paper, all controls, $u\colon [0, T] \to U$, are admissible.

In [2], it is shown that minimum wheel-rotation trajectories exist. The Pontryagin Maximum Principle [5] provides a necessary condition for optimality. Using the Pontryagin Maximum Principle, candidate trajectories are characterized in [2], and eventually, geometrical methods completely determine minimum wheel-rotation trajectories.

Def 1: An *extremal* is a trajectory $q(t)$ that satisfies the conditions of the Pontryagin Maximum Principle [2], [5].

III. Characterization of Extremals

In [2], two classes of extremals, *tight* and *loose*, are distinguished.

A. Tight Extremals

For every tight extremal there are two parallel lines ℓ_1 and ℓ_2 in the plane. The two lines ℓ_1 and ℓ_2 cut the plane into five disjoint subsets (see Figure 2): S_+, ℓ_1, $S_\pm$, ℓ_2, and S_-. Along the extremal, both wheels of the robot must stay on or between the two lines (see Figure 2). Furthermore, the extremal control law is

$$u_1 \in \begin{cases}[-1, 0] & \text{if wheel 2} \in \ell_1\\ \{0\} & \text{if wheel 2} \in S_\pm\\ [0, 1] & \text{if wheel 2} \in \ell_2\end{cases} \tag{5}$$

$$u_2 \in \begin{cases}[0, 1] & \text{if wheel 1} \in \ell_1\\ \{0\} & \text{if wheel 1} \in S_\pm\\ [-1, 0] & \text{if wheel 1} \in \ell_2\end{cases}. \tag{6}$$

It can be seen from the above extremal control law that tight extremals are composed of swing and straight segments. We use $\mathbf{L}$, $\mathbf{R}$, and $\mathbf{S}$ to denote swing around the left wheel, the right wheel, and straight line motions respectively. We use a superscript for direction: $-$ is clockwise, $+$ is counter-clockwise, $+$ is forward, and $-$ is backward. Otherwise, the direction of swing is constant throughout the trajectory. The symbol * means zero or more copies of the base expression. Depending on the distance between ℓ_1 and ℓ_2 there are three different types of tight extremals. For each type, we define a finite state machine to present extremals more precisely.

Case 1: Let $d(\ell_1, \ell_2) = 2b$ in which d is the distance function. Besides swing, the robot can move straight forward and backward by keeping the wheels on ℓ_i's. In this case, the extremals are composed of a sequence of swing and straight segments. We define a finite state machine $\mathcal{F}_1$ to present such extremals more precisely. Let

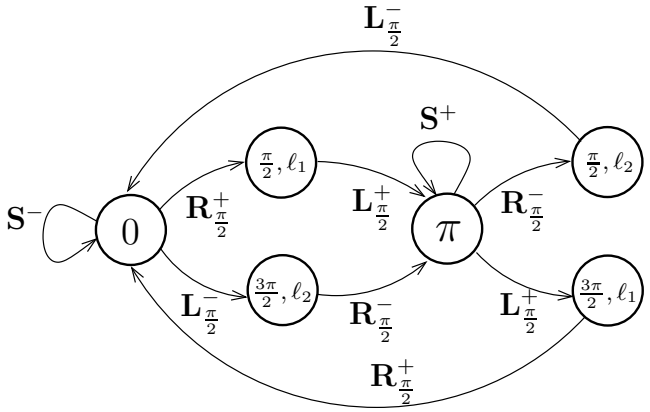

Fig. 3. $\mathcal{F}_1$ represents case 1 tight extremals

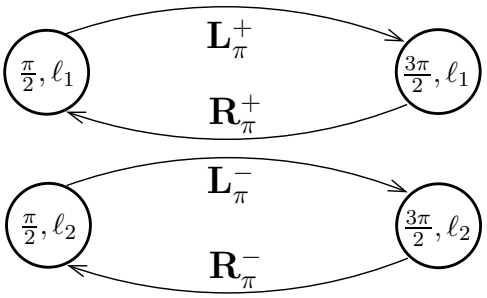

Fig. 4. $\mathcal{F}_2$ represents case 2 tight extremals

$Q_1 = \{0, (\frac{\pi}{2},\ell_1), (\frac{\pi}{2},\ell_2), \pi, (\frac{3\pi}{2},\ell_1), (\frac{3\pi}{2},\ell_2)\}$ be the set of states. States are the robot orientations together with its position, i.e. whether it lies on the line ℓ_1 or ℓ_2. Let the input alphabet be $\Sigma_1 = \{\mathbf{S}^+, \mathbf{S}^-, \mathbf{L}^+_{\frac{\pi}{2}}, \mathbf{L}^-_{\frac{\pi}{2}}, \mathbf{R}^+_{\frac{\pi}{2}}, \mathbf{R}^-_{\frac{\pi}{2}}\}$. Define $\mathcal{F}_1$ by the transition function that is depicted in Figure 3. If robot starts in one of the states in Q_1, it has to move according to $\mathcal{F}_1$. If the initial configuration of robot is none of the states, the robot performs a compliant $\mathbf{L}_\alpha$ or $\mathbf{R}_\alpha$ motion, in which $0 \leq \alpha < \frac{\pi}{2}$, to reach one the states and continues according to $\mathcal{F}_1$. In general, there can be an arbitrary number of swing and straight segments. Since the straight segments can be translated and merged together, a representative subclass with only one straight segment suffices for giving all such minimum wheel-rotation trajectories.

Case 2: Let $d(\ell_1, \ell_2) > 2b$. The robot cannot move straight because it cannot keep the wheels on ℓ_i's over some interval of time. Thus, such extremals are of the form $(\mathbf{R}_\pi \mathbf{L}_\pi)^*$. Note that these extremals are sub-paths of case 1 extremals. Again, we define a finite state machine $\mathcal{F}_2$ to present such extremals more precisely. Let $Q_2 = \{(\frac{\pi}{2},\ell_1), (\frac{\pi}{2},\ell_2), (\frac{3\pi}{2},\ell_1), (\frac{3\pi}{2},\ell_2)\}$ be the set of states. States are the robot orientations together with its position, i.e. whether it lies on the line ℓ_1 or ℓ_2. Let the input alphabet be $\Sigma_2 = \{\mathbf{L}^+_\pi, \mathbf{L}^-_\pi, \mathbf{R}^+_\pi, \mathbf{R}^-_\pi\}$. Define $\mathcal{F}_2$ by the transition function that is depicted in Figure 4.

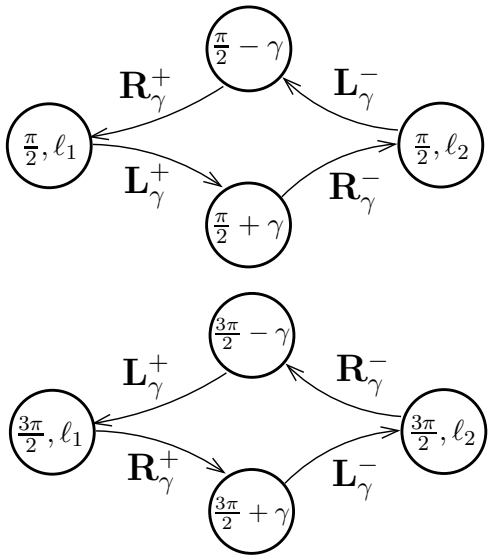

Fig. 5. $\mathcal{F}_3$ represents case 3 tight extremals

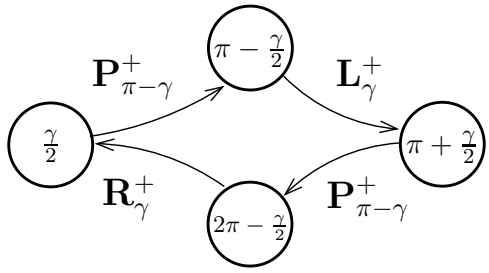

Fig. 6. $\mathcal{E}_1$ provides a representative subclass of loose extremals in $+$ direction.

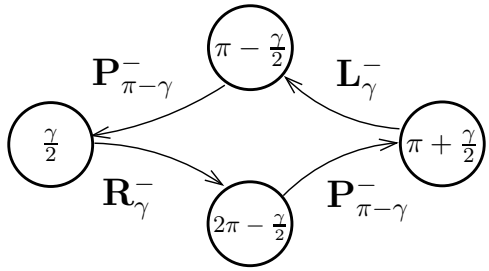

Fig. 7. $\mathcal{E}_2$ provides a representative subclass of loose extremals in $-$ direction.

Case 3: Let $d(\ell_1, \ell_2) < 2b$. In this case, the extremals are of the form $(\mathbf{L}^-_\gamma \mathbf{R}^-_\gamma \mathbf{L}^+_\gamma \mathbf{R}^+_\gamma)^*$ in which $\gamma = \sin^{-1}(d(\ell_1,\ell_2)/2b) < \frac{\pi}{2}$. Like the two previous cases, we define a finite state machine $\mathcal{F}_3$ to present such extremals more precisely. Let $Q_3 = \{\frac{\pi}{2}-\gamma, (\frac{\pi}{2},\ell_1), (\frac{\pi}{2},\ell_2), \frac{\pi}{2}+\gamma, \frac{3\pi}{2}-\gamma, (\frac{3\pi}{2},\ell_1), (\frac{3\pi}{2},\ell_2), \frac{3\pi}{2}+\gamma\}$ be the set of states. States are the robot orientations together with its position, i.e. whether it lies on the line ℓ_1 or ℓ_2. Let the input alphabet be $\Sigma_3 = \{\mathbf{L}^+_\gamma, \mathbf{L}^-_\gamma, \mathbf{R}^+_\gamma, \mathbf{R}^-_\gamma\}$. Define $\mathcal{F}_3$ by the transition function that is depicted in Figure 5.

Lemma 1 ([2]): Let $q(t)$ be a tight extremal. Wheel-rotation of q is the length of the projection of $q(t)$ onto the x-y plane.

B. Loose Extremals

The PMP does not give a restrictive enough extremal control law for loose extremals [2]. In fact, the only constraint the PMP imposes on loose extremals is that $u_1, -u_2 \in [0,1]$ or $u_1, -u_2 \in [-1,0]$. The following lemma shows that for those loose extremals that happen to be minimum wheel-rotation, there exists an equivalent trajectory (i.e. with equal wheel-rotation) with the same boundary points which is composed of swing and rotation in place.

Lemma 2 ([2]): Let $(q(t), u(t)) \in \mathcal{P}$ be a loose minimum wheel-rotation trajectory-control pair that tranfers the initial configuration q_i to the goal configuration q_g. There exists a trajectory-control pair $(\breve{q}(t), \breve{u}(t)) \in \mathcal{P}$ transferring q_i to q_g, in which $\breve{u}$ is composed of a sequence of alternating rotation in place and swing segments in the same direction. Furthermore, $q(t)$ and $\breve{q}(t)$ have the same wheel rotation, i.e. $J(u) = J(\breve{u})$.

We use $\mathbf{P}$ to denote rotation in place. In order to present the representative subclass of loose extremals whose existence is established in Lemma 2, we define finite state machines $\mathcal{E}_1$ and $\mathcal{E}_2$. Let $0 \leq \gamma \leq \pi$ and $Q = \{\frac{\gamma}{2}, \pi - \frac{\gamma}{2}, \pi + \frac{\gamma}{2}, 2\pi - \frac{\gamma}{2}\}$ be the set of states which represent the robot orientation. Let the input alphabet be $\Sigma = \{\mathbf{L}^+_\gamma, \mathbf{L}^-_\gamma, \mathbf{R}^+_\gamma, \mathbf{R}^-_\gamma, \mathbf{P}^+_{\pi-\gamma}, \mathbf{P}^-_{\pi-\gamma}\}$. Define $\mathcal{E}_1$ and $\mathcal{E}_2$ by the transition functions that are depicted in Figures 6 and 7 respectively. $\mathcal{E}_1$ provides a representative subclass of loose extremals in $+$ direction and $\mathcal{E}_2$ in $-$ direction.

Lemma 3 ([2]): Let $q(t)$ be a loose extremal associated with the control $u(t)$, and let ϑ be the length of the projection of $q(t)$ onto $\mathbb{S}^1$. In this case wheel-rotation of q is $b\vartheta$.

IV. Characterization of Maximal Minimum Wheel-Rotation Trajectories

In previous section, extremals which are candidate minimum wheel-rotation trajectories were studied. Using geometrical techniques, one can give a characterization of minimum wheel-rotation trajectories for differential-drive mobile robots. Particularly, since any sub-path of an optimal path is necessarily optimal, we presented minimum wheel-rotation trajectories that are maximal with respect to sub-path partial order in [2]. In the following, we precisely define sub-path partial order as well as symmetries of the problem, and we summarize minimum wheel-rotation trajectories that are maximal with repsect to sub-path partial order.

A. Sub-Path Partial Order

Let P be the set of all finite-time trajectory-control pairs of the differential-drive. More precisely,

$$P = \{(q,u) \mid \ q\colon [0,T] \to \mathcal{C}, u\colon [0,T] \to U, \ \dot{q} = f(q,u)\}. \tag{7}$$

In this paper, input functions are admissible, and those that are equal almost everywhere (a.e.) are assumed to be identical. Let (q,u) and (q',u') be two elements of P which are defined respectively on $[0,T]$ and $[0,T']$. In order to define sub-path relation, we give a partial order $\preceq$ on P. We define $(q,u) \preceq (q',u')$ iff

$$T \leq T' \text{ and } \exists\ \delta t \geq 0, \forall\ t \in [0,T], u(t) = u'(t+\delta t). \tag{8}$$

Define the relation $\sim$ on P as follows:

$$(q,u) \sim (q',u') \iff (q,u) \preceq (q',u') \text{ and } (q',u') \preceq (q,u). \tag{9}$$

Since $\sim$ is an equivalence relation, $\mathcal{P} = P/\!\sim$ is well-defined and is the set of all finite-time trajectory-control pairs of the differential-drive up to plane transformations. Since $\preceq$ is a partial order on P and $\sim$ is an equivalence relation, $\preceq$ is also a well-defined partial order on $\mathcal{P} = P/\!\sim$.

B. Symmetries

Assume $(q,u) \in \mathcal{P}$ is a minimum wheel-rotation trajectory-control pair that is defined on $[0,T]$. Let $\tilde{q}(t)$ be the trajectory associated with control $u(T-t)$, $\bar{q}(t)$ the trajectory associated with control $-u(t)$, and $\hat{q}(t)$ the trajectory associated with control $\hat{u}(t) = (u_2(t), u_1(t))$. Define the operators $\mathcal{O}_1$, $\mathcal{O}_2$, and $\mathcal{O}_3$ on $\mathcal{P}$ by

$$\mathcal{O}_1 : (q(t),u(t)) \ \mapsto \ (\tilde{q}(t), u(T-t)) \tag{10}$$

$$\mathcal{O}_2 : (q(t),u(t)) \ \mapsto \ (\bar{q}(t), -u(t)) \tag{11}$$

$$\mathcal{O}_3 : (q(t),u(t)) \ \mapsto \ (\hat{q}(t), \hat{u}(t)). \tag{12}$$

Due to symmetries, $\mathcal{O}_1(q,u)$, $\mathcal{O}_2(q,u)$, and $\mathcal{O}_3(q,u)$ are also minimum wheel-rotation trajectories. $\mathcal{O}_1$ corresponds to reversing the trajectory in time, $\mathcal{O}_2$ corresponds to reversing the inputs, and $\mathcal{O}_3$ corresponds to exchanging the left and the right wheels.

C. Optimal Trajectories That Are Maximal in $\mathcal{P}$

Minimum wheel-rotation trajectories are composed of a finite number of swing, straight, and rotation in place segments [2]. Let $\mathbf{L}$, $\mathbf{R}$, $\mathbf{S}$, $\mathbf{P}$, $-$, and $+$ be the same as in Section III. Subscripts are non-negative angles or distances. Here we summarize minimum wheel-rotation trajectories that are maximal with respect to the partial order $\preceq$ which is described in Section IV-A. Taking the symmetries in Section IV-B into account, all of the maximal minimum wheel-rotation trajectories, with their symmetric clones, are given in Table I. Since the symmetry operators $\mathcal{O}_1, \mathcal{O}_2$, and $\mathcal{O}_3$ commute, we do not need to worry about their order.

V. All Minimum Wheel-Rotation Trajectories

In order to determine the shortest path for every pair of initial and goal configurations, we need to characterize all of the minimum wheel-rotation trajectories regardless of whether they are maximal. Here we will give all of the minimum wheel-rotation trajectories. We will also compute their cost and goal configuration in terms of the parameters. Thus, finding the shortest path for every pair of initial and goal configurations reduces to solving systems of equations for the path parameters. In the following sections, symbols are the same as in Section III. Also $\mathbf{C}$ represents a swing, $\mathbf{L}$ or $\mathbf{R}$, and $|$ represents a change of direction. Note that in the following, orientation of the robot θ must always be

TABLE I

MAXIMAL MINIMUM WHEEL-ROTATION TRAJECTORIES SORTED BY SYMMETRY CLASS

	(A)	(B)
Base	$\mathbf{L}_\alpha^-\mathbf{R}_{\frac{\pi}{2}}^-\mathbf{S}^+\mathbf{R}_\beta^-$	$\mathbf{L}_\alpha^-\mathbf{R}_{\frac{\pi}{2}}^-\mathbf{S}^+\mathbf{L}_{\frac{\pi}{2}}^+\mathbf{R}_\beta^+$
$\mathcal{O}_1$	$\mathbf{R}_\beta^-\mathbf{S}^+\mathbf{R}_{\frac{\pi}{2}}^-\mathbf{L}_\alpha^-$	$\mathbf{R}_\beta^+\mathbf{L}_{\frac{\pi}{2}}^+\mathbf{S}^+\mathbf{R}_{\frac{\pi}{2}}^-\mathbf{L}_\alpha^-$
$\mathcal{O}_2$	$\mathbf{L}_\alpha^+\mathbf{R}_{\frac{\pi}{2}}^+\mathbf{S}^-\mathbf{R}_\beta^+$	$\mathbf{L}_\alpha^+\mathbf{R}_{\frac{\pi}{2}}^+\mathbf{S}^-\mathbf{L}_{\frac{\pi}{2}}^-\mathbf{R}_\beta^-$
$\mathcal{O}_3$	$\mathbf{R}_\alpha^+\mathbf{L}_{\frac{\pi}{2}}^+\mathbf{S}^+\mathbf{L}_\beta^+$	$\mathbf{R}_\alpha^+\mathbf{L}_{\frac{\pi}{2}}^+\mathbf{S}^+\mathbf{R}_{\frac{\pi}{2}}^-\mathbf{L}_\beta^-$
$\mathcal{O}_1\circ\mathcal{O}_2$	$\mathbf{R}_\beta^+\mathbf{S}^-\mathbf{R}_{\frac{\pi}{2}}^+\mathbf{L}_\alpha^+$	$\mathbf{R}_\beta^-\mathbf{L}_{\frac{\pi}{2}}^-\mathbf{S}^-\mathbf{R}_{\frac{\pi}{2}}^+\mathbf{L}_\alpha^+$
$\mathcal{O}_1\circ\mathcal{O}_3$	$\mathbf{L}_\beta^+\mathbf{S}^+\mathbf{L}_{\frac{\pi}{2}}^+\mathbf{R}_\alpha^+$	$\mathbf{L}_\beta^-\mathbf{R}_{\frac{\pi}{2}}^-\mathbf{S}^+\mathbf{L}_{\frac{\pi}{2}}^+\mathbf{R}_\alpha^+$
$\mathcal{O}_2\circ\mathcal{O}_3$	$\mathbf{R}_\alpha^-\mathbf{L}_{\frac{\pi}{2}}^-\mathbf{S}^-\mathbf{L}_\beta^-$	$\mathbf{R}_\alpha^-\mathbf{L}_{\frac{\pi}{2}}^-\mathbf{S}^-\mathbf{R}_{\frac{\pi}{2}}^+\mathbf{L}_\beta^+$
$\mathcal{O}_1\circ\mathcal{O}_2\circ\mathcal{O}_3$	$\mathbf{L}_\beta^-\mathbf{S}^-\mathbf{L}_{\frac{\pi}{2}}^-\mathbf{R}_\alpha^-$	$\mathbf{L}_\beta^+\mathbf{R}_{\frac{\pi}{2}}^+\mathbf{S}^-\mathbf{L}_{\frac{\pi}{2}}^-\mathbf{R}_\alpha^-$
	$\alpha+\beta\leq\frac{\pi}{2}$	$\alpha+\beta\leq 2$

	(C)	(D)
Base	$\mathbf{L}_\alpha^-\mathbf{R}_\gamma^-\mathbf{L}_\gamma^+\mathbf{R}_\beta^+$	$\mathbf{L}_\alpha^+\mathbf{R}_\gamma^-\mathbf{L}_\gamma^-\mathbf{R}_\beta^+$
$\mathcal{O}_1$	$\mathbf{R}_\beta^+\mathbf{L}_\gamma^+\mathbf{R}_\gamma^-\mathbf{L}_\alpha^-$	$\mathbf{R}_\beta^+\mathbf{L}_\gamma^-\mathbf{R}_\gamma^-\mathbf{L}_\alpha^+$
$\mathcal{O}_2$	$\mathbf{L}_\alpha^+\mathbf{R}_\gamma^+\mathbf{L}_\gamma^-\mathbf{R}_\beta^-$	$\mathbf{L}_\alpha^-\mathbf{R}_\gamma^+\mathbf{L}_\gamma^+\mathbf{R}_\beta^-$
$\mathcal{O}_3$	$\mathbf{R}_\alpha^+\mathbf{L}_\gamma^+\mathbf{R}_\gamma^-\mathbf{L}_\beta^-$	$\mathbf{R}_\alpha^-\mathbf{L}_\gamma^+\mathbf{R}_\gamma^+\mathbf{L}_\beta^-$
$\mathcal{O}_1\circ\mathcal{O}_2$	$\mathbf{R}_\beta^-\mathbf{L}_\gamma^-\mathbf{R}_\gamma^+\mathbf{L}_\alpha^+$	$\mathbf{R}_\beta^-\mathbf{L}_\gamma^+\mathbf{R}_\gamma^+\mathbf{L}_\alpha^-$
$\mathcal{O}_1\circ\mathcal{O}_3$	$\mathbf{L}_\beta^-\mathbf{R}_\gamma^-\mathbf{L}_\gamma^+\mathbf{R}_\alpha^+$	$\mathbf{L}_\beta^-\mathbf{R}_\gamma^+\mathbf{L}_\gamma^+\mathbf{R}_\alpha^-$
$\mathcal{O}_2\circ\mathcal{O}_3$	$\mathbf{R}_\alpha^-\mathbf{L}_\gamma^-\mathbf{R}_\gamma^+\mathbf{L}_\beta^+$	$\mathbf{R}_\alpha^+\mathbf{L}_\gamma^-\mathbf{R}_\gamma^-\mathbf{L}_\beta^+$
$\mathcal{O}_1\circ\mathcal{O}_2\circ\mathcal{O}_3$	$\mathbf{L}_\beta^+\mathbf{R}_\gamma^+\mathbf{L}_\gamma^-\mathbf{R}_\alpha^-$	$\mathbf{L}_\beta^+\mathbf{R}_\gamma^-\mathbf{L}_\gamma^-\mathbf{R}_\alpha^+$
	$\alpha,\beta<\gamma\leq\frac{\pi}{2}$	$\alpha,\beta<\gamma\leq\frac{\pi}{2}$

	(E)	(F)
Base	$\mathbf{R}_\alpha^+\mathbf{P}_\gamma^+\mathbf{L}_\beta^+$	$\mathbf{P}_\alpha^+\mathbf{R}_\gamma^+\mathbf{P}_\beta^+$
$\mathcal{O}_1$	$\mathbf{L}_\beta^+\mathbf{P}_\gamma^+\mathbf{R}_\alpha^+$	$\mathbf{P}_\beta^+\mathbf{R}_\gamma^+\mathbf{P}_\alpha^+$
$\mathcal{O}_2$	$\mathbf{R}_\alpha^-\mathbf{P}_\gamma^-\mathbf{L}_\beta^-$	$\mathbf{P}_\alpha^-\mathbf{R}_\gamma^-\mathbf{P}_\beta^-$
$\mathcal{O}_3$	$\mathbf{L}_\alpha^-\mathbf{P}_\gamma^-\mathbf{R}_\beta^-$	$\mathbf{P}_\alpha^-\mathbf{L}_\gamma^-\mathbf{P}_\beta^-$
$\mathcal{O}_1\circ\mathcal{O}_2$	$\mathbf{L}_\beta^-\mathbf{P}_\gamma^-\mathbf{R}_\alpha^-$	$\mathbf{P}_\beta^-\mathbf{R}_\gamma^-\mathbf{P}_\alpha^-$
$\mathcal{O}_1\circ\mathcal{O}_3$	$\mathbf{R}_\beta^-\mathbf{P}_\gamma^-\mathbf{L}_\alpha^-$	$\mathbf{P}_\beta^-\mathbf{L}_\gamma^-\mathbf{P}_\alpha^-$
$\mathcal{O}_2\circ\mathcal{O}_3$	$\mathbf{L}_\alpha^+\mathbf{P}_\gamma^+\mathbf{R}_\beta^+$	$\mathbf{P}_\alpha^+\mathbf{L}_\gamma^+\mathbf{P}_\beta^+$
$\mathcal{O}_1\circ\mathcal{O}_2\circ\mathcal{O}_3$	$\mathbf{R}_\beta^+\mathbf{P}_\gamma^+\mathbf{L}_\alpha^+$	$\mathbf{P}_\beta^+\mathbf{L}_\gamma^+\mathbf{P}_\alpha^+$
	$\alpha+\gamma+\beta\leq\pi$	$\alpha+\gamma+\beta\leq\pi$

considered an element of $\mathbb{S}^1$. In other words, θ is evaluated mod 2π.

Let the initial configuration of an arbitrary trajectory $q(t)$ be $(x_i, y_i, \theta_i) \in \mathcal{C}$, i.e. $q(0) = (x_i, y_i, \theta_i)$. Suppose $(q, u) \in \mathcal{P}$, and it is defined on $[0, T]$. Let $\hat{q}(t)$ be the trajectory corresponding to the input $u(t)$ such that $\hat{q}(0) = (0, 0, 0)$. Suppose the goal configuration of $\hat{q}$ is (x, y, θ), i.e. $\hat{q}(T) = (x, y, \theta)$. In that case, the goal configuration of q is

$$\begin{aligned} x_g &= x_i + x\cos\theta_i - y\sin\theta_i && (13)\\ y_g &= y_i + x\sin\theta_i + y\cos\theta_i && (14)\\ \theta_g &= \theta_i + \theta, && (15)\end{aligned}$$

i.e. $q(T) = (x_g, y_g, \theta_g)$. Thus, we may assume without loss of generality that the initial configuration of robot is $(0, 0, 0)$ throughout this section.

A. $\mathbf{C}_\alpha\mathbf{P}_\gamma\mathbf{C}_\beta$ and $\mathbf{P}_\alpha\mathbf{C}_\gamma\mathbf{P}_\beta$

In Table II, the list of minimum wheel-rotation trajectories of type $\mathbf{C}_\alpha\mathbf{P}_\gamma\mathbf{C}_\beta$ and $\mathbf{P}_\alpha\mathbf{C}_\gamma\mathbf{P}_\beta$ can be found. The goal configuration of $\mathbf{C}_\alpha\mathbf{P}_\gamma\mathbf{C}_\beta$ is

$$\begin{aligned} x &= -c(\sin\kappa_1 + \sin\kappa_2 - \sin\kappa_3) && (16)\\ y &= c(\cos\kappa_1 - 1 + \cos\kappa_2 - \cos\kappa_3) && (17)\\ \theta &= \kappa_3, && (18)\end{aligned}$$

and the goal configuration of $\mathbf{P}_\alpha\mathbf{C}_\gamma\mathbf{P}_\beta$ is

$$\begin{aligned} x &= c(\sin\kappa_1 - \sin\kappa_2) && (19)\\ y &= c(\cos\kappa_2 - \cos\kappa_1) && (20)\\ \theta &= \kappa_3, && (21)\end{aligned}$$

in which $\kappa_1, \kappa_2, \kappa_3$, and c are the parameters in Table II. Wheel-rotation of such trajectories is $\alpha + \gamma + \beta$.

TABLE II

$\alpha+\gamma+\beta\leq\pi$

$\mathbf{C}_\alpha\mathbf{P}_\gamma\mathbf{C}_\beta$	$\mathbf{P}_\alpha\mathbf{C}_\gamma\mathbf{P}_\beta$	κ_1	κ_2	κ_3	c
$\mathbf{R}_\alpha^+\mathbf{P}_\gamma^+\mathbf{L}_\beta^+$	$\mathbf{P}_\alpha^+\mathbf{R}_\gamma^+\mathbf{P}_\beta^+$	α	$\alpha+\gamma$	$\alpha+\gamma+\beta$	b
$\mathbf{L}_\alpha^+\mathbf{P}_\gamma^+\mathbf{R}_\beta^+$	$\mathbf{P}_\alpha^+\mathbf{L}_\gamma^+\mathbf{P}_\beta^+$	α	$\alpha+\gamma$	$\alpha+\gamma+\beta$	$-b$
$\mathbf{R}_\alpha^-\mathbf{P}_\gamma^-\mathbf{L}_\beta^-$	$\mathbf{P}_\alpha^-\mathbf{R}_\gamma^-\mathbf{P}_\beta^-$	$-\alpha$	$-\alpha-\gamma$	$-\alpha-\gamma-\beta$	b
$\mathbf{L}_\alpha^-\mathbf{P}_\gamma^-\mathbf{R}_\beta^-$	$\mathbf{P}_\alpha^-\mathbf{L}_\gamma^-\mathbf{P}_\beta^-$	$-\alpha$	$-\alpha-\gamma$	$-\alpha-\gamma-\beta$	$-b$

TABLE III

$\alpha,\beta\leq\gamma\leq\frac{\pi}{2}$

$\mathbf{C}_\alpha\vert\mathbf{C}_\gamma\mathbf{C}_\beta$	κ_1	κ_2	κ_3	c
$\mathbf{R}_\alpha^+\mathbf{L}_\gamma^-\mathbf{R}_\beta^-$	α	$\alpha-\gamma$	$\alpha-\gamma-\beta$	b
$\mathbf{L}_\alpha^+\mathbf{R}_\gamma^-\mathbf{L}_\beta^-$	α	$\alpha-\gamma$	$\alpha-\gamma-\beta$	$-b$
$\mathbf{R}_\alpha^-\mathbf{L}_\gamma^+\mathbf{R}_\beta^+$	$-\alpha$	$-\alpha+\gamma$	$-\alpha+\gamma+\beta$	b
$\mathbf{L}_\alpha^-\mathbf{R}_\gamma^+\mathbf{L}_\beta^+$	$-\alpha$	$-\alpha+\gamma$	$-\alpha+\gamma+\beta$	$-b$
$\mathbf{C}_\alpha\mathbf{C}_\gamma\vert\mathbf{C}_\beta$	κ_1	κ_2	κ_3	c
$\mathbf{R}_\alpha^+\mathbf{L}_\gamma^+\mathbf{R}_\beta^-$	α	$\alpha+\gamma$	$\alpha+\gamma-\beta$	b
$\mathbf{L}_\alpha^+\mathbf{R}_\gamma^+\mathbf{L}_\beta^-$	α	$\alpha+\gamma$	$\alpha+\gamma-\beta$	$-b$
$\mathbf{R}_\alpha^-\mathbf{L}_\gamma^-\mathbf{R}_\beta^+$	$-\alpha$	$-\alpha-\gamma$	$-\alpha-\gamma+\beta$	b
$\mathbf{L}_\alpha^-\mathbf{R}_\gamma^-\mathbf{L}_\beta^+$	$-\alpha$	$-\alpha-\gamma$	$-\alpha-\gamma+\beta$	$-b$

B. $\mathbf{C}_\alpha\vert\mathbf{C}_\gamma\mathbf{C}_\beta$ and $\mathbf{C}_\alpha\mathbf{C}_\gamma\vert\mathbf{C}_\beta$

In Table III, the list of minimum wheel-rotation trajectories of type $\mathbf{C}_\alpha\vert\mathbf{C}_\gamma\mathbf{C}_\beta$ and $\mathbf{C}_\alpha\mathbf{C}_\gamma\vert\mathbf{C}_\beta$ can be found. The goal configuration of both $\mathbf{C}_\alpha\vert\mathbf{C}_\gamma\mathbf{C}_\beta$ and $\mathbf{C}_\alpha\mathbf{C}_\gamma\vert\mathbf{C}_\beta$ is

$$\begin{aligned} x &= -c(2\sin\kappa_1 - 2\sin\kappa_2 + \sin\kappa_3) && (22)\\ y &= c(2\cos\kappa_1 - 1 - 2\cos\kappa_2 + \cos\kappa_3) && (23)\\ \theta &= \kappa_3, && (24)\end{aligned}$$

in which $\kappa_1, \kappa_2, \kappa_3$, and c are the parameters in Table III. Wheel-rotation of such trajectories is $\alpha + \gamma + \beta$.

C. $\mathbf{C}_\alpha\mathbf{C}_\gamma\vert\mathbf{C}_\gamma\mathbf{C}_\beta$ and $\mathbf{C}_\alpha\vert\mathbf{C}_\gamma\mathbf{C}_\gamma\vert\mathbf{C}_\beta$

In Table IV, the list of minimum wheel-rotation trajectories of type $\mathbf{C}_\alpha\mathbf{C}_\gamma\vert\mathbf{C}_\gamma\mathbf{C}_\beta$ and $\mathbf{C}_\alpha\vert\mathbf{C}_\gamma\mathbf{C}_\gamma\vert\mathbf{C}_\beta$ can be found.

TABLE IV

$\alpha, \beta \leq \gamma \leq \frac{\pi}{2}$

$\mathbf{C}_\alpha\mathbf{C}_\gamma\|\mathbf{C}_\gamma\mathbf{C}_\beta$	κ_1	κ_2	κ_3	c
$\mathbf{R}_\alpha^+\mathbf{L}_\gamma^+\mathbf{R}_\gamma^-\mathbf{L}_\beta^-$	α	$\alpha+\gamma$	$\alpha-\beta$	b
$\mathbf{L}_\alpha^+\mathbf{R}_\gamma^+\mathbf{L}_\gamma^-\mathbf{R}_\beta^-$	α	$\alpha+\gamma$	$\alpha-\beta$	$-b$
$\mathbf{R}_\alpha^-\mathbf{L}_\gamma^-\mathbf{R}_\gamma^+\mathbf{L}_\beta^+$	$-\alpha$	$-\alpha-\gamma$	$-\alpha+\beta$	b
$\mathbf{L}_\alpha^-\mathbf{R}_\gamma^-\mathbf{L}_\gamma^+\mathbf{R}_\beta^+$	$-\alpha$	$-\alpha-\gamma$	$-\alpha+\beta$	$-b$

$\mathbf{C}_\alpha\|\mathbf{C}_\gamma\mathbf{C}_\gamma\|\mathbf{C}_\beta$	κ_1	κ_2	κ_3	κ_4	c
$\mathbf{R}_\alpha^+\mathbf{L}_\gamma^-\mathbf{R}_\gamma^-\mathbf{L}_\beta^+$	α	$\alpha-\gamma$	$\alpha-2\gamma$	$\alpha-2\gamma+\beta$	b
$\mathbf{L}_\alpha^+\mathbf{R}_\gamma^-\mathbf{L}_\gamma^-\mathbf{R}_\beta^+$	α	$\alpha-\gamma$	$\alpha-2\gamma$	$\alpha-2\gamma+\beta$	$-b$
$\mathbf{R}_\alpha^-\mathbf{L}_\gamma^+\mathbf{R}_\gamma^+\mathbf{L}_\beta^-$	$-\alpha$	$-\alpha+\gamma$	$-\alpha+2\gamma$	$-\alpha+2\gamma-\beta$	b
$\mathbf{L}_\alpha^-\mathbf{R}_\gamma^+\mathbf{L}_\gamma^+\mathbf{R}_\beta^-$	$-\alpha$	$-\alpha+\gamma$	$-\alpha+2\gamma$	$-\alpha+2\gamma-\beta$	$-b$

TABLE V

$\alpha, \beta \leq \frac{\pi}{2}$ AND $d \geq 0$

$\mathbf{C}_\alpha\mathbf{S}_d\mathbf{C}_\beta$	κ_1	κ_2	c_1	c_2	c_3	c_4
$\mathbf{R}_\alpha^+\mathbf{S}_d^-\mathbf{R}_\beta^+$	α	$\alpha+\beta$	$-d$	0	$-b$	$-b$
$\mathbf{L}_\alpha^+\mathbf{S}_d^+\mathbf{L}_\beta^+$	α	$\alpha+\beta$	d	0	b	b
$\mathbf{R}_\alpha^+\mathbf{S}_d^-\mathbf{L}_\beta^-$	α	$\alpha-\beta$	$-d$	$-2b$	b	$-b$
$\mathbf{L}_\alpha^+\mathbf{S}_d^+\mathbf{R}_\beta^-$	α	$\alpha-\beta$	d	$2b$	$-b$	b
$\mathbf{R}_\alpha^-\mathbf{S}_d^+\mathbf{R}_\beta^-$	$-\alpha$	$-\alpha-\beta$	d	0	$-b$	$-b$
$\mathbf{L}_\alpha^-\mathbf{S}_d^-\mathbf{L}_\beta^-$	$-\alpha$	$-\alpha-\beta$	$-d$	0	b	b
$\mathbf{R}_\alpha^-\mathbf{S}_d^+\mathbf{L}_\beta^+$	$-\alpha$	$-\alpha+\beta$	d	$-2b$	b	$-b$
$\mathbf{L}_\alpha^-\mathbf{S}_d^-\mathbf{R}_\beta^+$	$-\alpha$	$-\alpha+\beta$	$-d$	$2b$	$-b$	b

The goal configuration of $\mathbf{C}_\alpha\mathbf{C}_\gamma|\mathbf{C}_\gamma\mathbf{C}_\beta$ is

$$x = -c(4\sin\kappa_1 - 2\sin\kappa_2 - \sin\kappa_3) \quad (25)$$
$$y = c(4\cos\kappa_1 - 1 - 2\cos\kappa_2 - \cos\kappa_3) \quad (26)$$
$$\theta = \kappa_3, \quad (27)$$

and the goal configuration of $\mathbf{C}_\alpha|\mathbf{C}_\gamma\mathbf{C}_\gamma|\mathbf{C}_\beta$ is

$$x = -c(2\sin\kappa_1 - 2\sin\kappa_2 + 2\sin\kappa_3 - \sin\kappa_4) \quad (28)$$
$$y = c(2\cos\kappa_1 - 1 - 2\cos\kappa_2 + 2\cos\kappa_3 - \cos\kappa_4) \quad (29)$$
$$\theta = \kappa_4, \quad (30)$$

in which $\kappa_1, \kappa_2, \kappa_3, \kappa_4$, and c are the parameters in Table IV. Wheel-rotation of such trajectories is $\alpha + 2\gamma + \beta$.

D. $\mathbf{C}_\alpha\mathbf{S}_d\mathbf{C}_\beta$

In Table V, the list of minimum wheel-rotation trajectories of type $\mathbf{C}_\alpha\mathbf{S}_d\mathbf{C}_\beta$ can be found. The goal configuration of $\mathbf{C}_\alpha\mathbf{S}_d\mathbf{C}_\beta$ is

$$x = c_1\cos\kappa_1 + c_2\sin\kappa_1 + c_3\sin\kappa_2 \quad (31)$$
$$y = c_1\sin\kappa_1 - c_2\cos\kappa_1 - c_3\cos\kappa_2 + c_4 \quad (32)$$
$$\theta = \kappa_2, \quad (33)$$

in which $\kappa_1, \kappa_2, c_1, c_2, c_3$, and c_4 are the parameters in Table V. Wheel-rotation of such trajectories is $\alpha + d + \beta$.

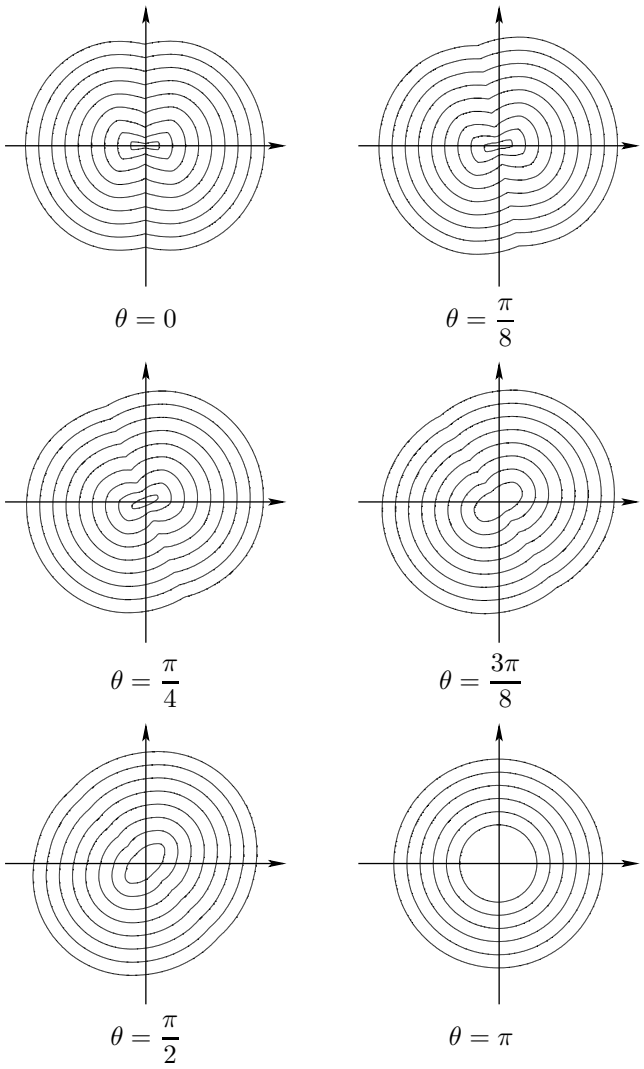

Fig. 8. Level sets of the cost-to-go function for $\theta = 0, \frac{\pi}{8}, \frac{\pi}{4}, \frac{3\pi}{8}, \frac{\pi}{2}$, and π

E. $\mathbf{C}_\alpha\mathbf{C}_{\frac{\pi}{2}}\mathbf{S}_d\mathbf{C}_\beta$ *and* $\mathbf{C}_\alpha\mathbf{S}_d\mathbf{C}_{\frac{\pi}{2}}\mathbf{C}_\beta$

In Table VI, the list of minimum wheel-rotation trajectories of type $\mathbf{C}_\alpha\mathbf{C}_{\frac{\pi}{2}}\mathbf{S}_d\mathbf{C}_\beta$ and $\mathbf{C}_\alpha\mathbf{S}_d\mathbf{C}_{\frac{\pi}{2}}\mathbf{C}_\beta$ can be found. The goal configuration of such trajectories is

$$x = c_1\sin\kappa_1 + c_2\cos\kappa_1 + c_3\sin\kappa_2 \quad (34)$$
$$y = -c_1\cos\kappa_1 + c_2\sin\kappa_1 - c_3\cos\kappa_2 + c_4 \quad (35)$$
$$\theta = \kappa_2, \quad (36)$$

in which $\kappa_1, \kappa_2, c_1, c_2, c_3$, and c_4 are the parameters in Table VI. Wheel-rotation of such trajectories is $\alpha + \frac{\pi}{2} + d + \beta$.

F. $\mathbf{L}_\alpha\mathbf{R}_{\frac{\pi}{2}}\mathbf{S}_d\mathbf{L}_{\frac{\pi}{2}}\mathbf{R}_\beta$ *and* $\mathbf{R}_\alpha\mathbf{L}_{\frac{\pi}{2}}\mathbf{S}_d\mathbf{R}_{\frac{\pi}{2}}\mathbf{L}_\beta$

In Table VII, the list of minimum wheel-rotation trajectories of type $\mathbf{L}_\alpha\mathbf{R}_{\frac{\pi}{2}}\mathbf{S}_d\mathbf{L}_{\frac{\pi}{2}}\mathbf{R}_\beta$ and $\mathbf{R}_\alpha\mathbf{L}_{\frac{\pi}{2}}\mathbf{S}_d\mathbf{R}_{\frac{\pi}{2}}\mathbf{L}_\beta$ can be found. The goal configuration of such trajectories is

$$x = c_1\sin\kappa_1 + c_2\cos\kappa_1 + c_3\sin\kappa_2 \quad (37)$$
$$y = -c_1\cos\kappa_1 + c_2\sin\kappa_1 - c_3\cos\kappa_2 - c_3 \quad (38)$$
$$\theta = \kappa_2, \quad (39)$$

TABLE VI

$d \geq 0$

Range	$\mathbf{C}_\alpha \mathbf{C}_{\frac{\pi}{2}} \mathbf{S}_d \mathbf{C}_\beta$	κ_1	κ_2	c_1	c_2	c_3	c_4
$\alpha, \beta \leq \frac{\pi}{2}$	$\mathbf{R}_\alpha^+ \mathbf{L}_{\frac{\pi}{2}}^+ \mathbf{S}_d^+ \mathbf{R}_\beta^-$	α	$\alpha + \frac{\pi}{2} - \beta$	$-2b - d$	$2b$	$-b$	$-b$
$\alpha, \beta \leq \frac{\pi}{2}$	$\mathbf{L}_\alpha^+ \mathbf{R}_{\frac{\pi}{2}}^+ \mathbf{S}_d^- \mathbf{L}_\beta^-$	α	$\alpha + \frac{\pi}{2} - \beta$	$2b + d$	$-2b$	b	b
$\alpha + \beta \leq \frac{\pi}{2}$	$\mathbf{R}_\alpha^+ \mathbf{L}_{\frac{\pi}{2}}^+ \mathbf{S}_d^+ \mathbf{L}_\beta^+$	α	$\alpha + \frac{\pi}{2} + \beta$	$-2b - d$	0	b	$-b$
$\alpha + \beta \leq \frac{\pi}{2}$	$\mathbf{L}_\alpha^+ \mathbf{R}_{\frac{\pi}{2}}^+ \mathbf{S}_d^- \mathbf{R}_\beta^+$	α	$\alpha + \frac{\pi}{2} + \beta$	$2b + d$	0	$-b$	b
$\alpha, \beta \leq \frac{\pi}{2}$	$\mathbf{R}_\alpha^- \mathbf{L}_{\frac{\pi}{2}}^- \mathbf{S}_d^- \mathbf{R}_\beta^+$	$-\alpha$	$-\alpha - \frac{\pi}{2} + \beta$	$-2b - d$	$-2b$	$-b$	$-b$
$\alpha, \beta \leq \frac{\pi}{2}$	$\mathbf{L}_\alpha^- \mathbf{R}_{\frac{\pi}{2}}^- \mathbf{S}_d^+ \mathbf{L}_\beta^+$	$-\alpha$	$-\alpha - \frac{\pi}{2} + \beta$	$2b + d$	$2b$	b	b
$\alpha + \beta \leq \frac{\pi}{2}$	$\mathbf{R}_\alpha^- \mathbf{L}_{\frac{\pi}{2}}^- \mathbf{S}_d^- \mathbf{L}_\beta^-$	$-\alpha$	$-\alpha - \frac{\pi}{2} - \beta$	$-2b - d$	0	b	$-b$
$\alpha + \beta \leq \frac{\pi}{2}$	$\mathbf{L}_\alpha^- \mathbf{R}_{\frac{\pi}{2}}^- \mathbf{S}_d^+ \mathbf{R}_\beta^-$	$-\alpha$	$-\alpha - \frac{\pi}{2} - \beta$	$2b + d$	0	$-b$	b
Range	$\mathbf{C}_\alpha \mathbf{S}_d \mathbf{C}_{\frac{\pi}{2}} \mathbf{C}_\beta$	κ_1	κ_2	c_1	c_2	c_3	c_4
$\alpha, \beta \leq \frac{\pi}{2}$	$\mathbf{R}_\alpha^+ \mathbf{S}_d^- \mathbf{L}_{\frac{\pi}{2}}^- \mathbf{R}_\beta^-$	α	$\alpha - \frac{\pi}{2} - \beta$	$-2b$	$-2b - d$	$-b$	$-b$
$\alpha, \beta \leq \frac{\pi}{2}$	$\mathbf{L}_\alpha^+ \mathbf{S}_d^+ \mathbf{R}_{\frac{\pi}{2}}^- \mathbf{L}_\beta^-$	α	$\alpha - \frac{\pi}{2} - \beta$	$2b$	$2b + d$	b	b
$\alpha + \beta \leq \frac{\pi}{2}$	$\mathbf{R}_\alpha^+ \mathbf{S}_d^- \mathbf{R}_{\frac{\pi}{2}}^+ \mathbf{L}_\beta^+$	α	$\alpha + \frac{\pi}{2} + \beta$	0	$-2b - d$	b	$-b$
$\alpha + \beta \leq \frac{\pi}{2}$	$\mathbf{L}_\alpha^+ \mathbf{S}_d^+ \mathbf{L}_{\frac{\pi}{2}}^+ \mathbf{R}_\beta^+$	α	$\alpha + \frac{\pi}{2} + \beta$	0	$2b + d$	$-b$	b
$\alpha, \beta \leq \frac{\pi}{2}$	$\mathbf{R}_\alpha^- \mathbf{S}_d^+ \mathbf{L}_{\frac{\pi}{2}}^+ \mathbf{R}_\beta^+$	$-\alpha$	$-\alpha + \frac{\pi}{2} + \beta$	$-2b$	$2b + d$	$-b$	$-b$
$\alpha, \beta \leq \frac{\pi}{2}$	$\mathbf{L}_\alpha^- \mathbf{S}_d^- \mathbf{R}_{\frac{\pi}{2}}^+ \mathbf{L}_\beta^+$	$-\alpha$	$-\alpha + \frac{\pi}{2} + \beta$	$2b$	$-2b - d$	b	b
$\alpha + \beta \leq \frac{\pi}{2}$	$\mathbf{R}_\alpha^- \mathbf{S}_d^+ \mathbf{R}_{\frac{\pi}{2}}^- \mathbf{L}_\beta^-$	$-\alpha$	$-\alpha - \frac{\pi}{2} - \beta$	0	$2b + d$	b	$-b$
$\alpha + \beta \leq \frac{\pi}{2}$	$\mathbf{L}_\alpha^- \mathbf{S}_d^- \mathbf{L}_{\frac{\pi}{2}}^- \mathbf{R}_\beta^-$	$-\alpha$	$-\alpha - \frac{\pi}{2} - \beta$	0	$-2b - d$	$-b$	b

TABLE VII

$\alpha + \beta < 2$ AND $d \geq 0$

$\mathbf{C}_\alpha \mathbf{C}_{\frac{\pi}{2}} \mathbf{S}_d \mathbf{C}_{\frac{\pi}{2}} \mathbf{C}_\beta$	κ_1	κ_2	c_1	c_2	c_3
$\mathbf{R}_\alpha^+ \mathbf{L}_{\frac{\pi}{2}}^+ \mathbf{S}_d^+ \mathbf{R}_{\frac{\pi}{2}}^- \mathbf{L}_\beta^-$	α	$\alpha - \beta$	$-4b - d$	$2b$	b
$\mathbf{L}_\alpha^+ \mathbf{R}_{\frac{\pi}{2}}^+ \mathbf{S}_d^- \mathbf{L}_{\frac{\pi}{2}}^- \mathbf{R}_\beta^-$	α	$\alpha - \beta$	$4b + d$	$-2b$	$-b$
$\mathbf{R}_\alpha^- \mathbf{L}_{\frac{\pi}{2}}^- \mathbf{S}_d^- \mathbf{R}_{\frac{\pi}{2}}^+ \mathbf{L}_\beta^+$	$-\alpha$	$-\alpha + \beta$	$-4b - d$	$-2b$	b
$\mathbf{L}_\alpha^- \mathbf{R}_{\frac{\pi}{2}}^- \mathbf{S}_d^+ \mathbf{L}_{\frac{\pi}{2}}^+ \mathbf{R}_\beta^+$	$-\alpha$	$-\alpha + \beta$	$4b + d$	$2b$	$-b$

in which $\kappa_1, \kappa_2, c_1, c_2$, and c_3 are the parameters in Table VII. Wheel-rotation of such trajectories is $\alpha + \pi + d + \beta$.

VI. Cost-to-go Function

In Figure 8, level sets of the cost-to-go function for some goal orientations are presented. In computing the cost-to-go function, initial configuration is assumed to be $(0, 0, 0)$, and goal orientation θ is assumed to be 0, $\frac{\pi}{8}$, $\frac{\pi}{4}$, $\frac{3\pi}{8}$, $\frac{\pi}{2}$, and π.

Numerical computations show that minimum wheel-rotation cost-to-go function is similar to Reeds-Shepp cost-to-go function. Moreover, a collection of Reeds-Shepp curves are among minimum wheel-rotation trajectories. This may suggest that minimum wheel-rotation cost-to-go function is equal to Reeds-Shepp cost-to-go function. However, minimum wheel-rotation trajectories are different from Reeds-Shepp curves because there are minimum wheel-rotation trajectories that contain rotation in place.

VII. Conclusions

We presented finite state machines for different categories of extremals. We then summarized maximal minimum wheel-rotation trajectories. Using previous characterization of maximal minimum wheel-rotation trajectories in [2], we derived 52 different minimum wheel-rotation trajectories, which are listed in Section V. We further determined the end-point map in terms of the parameters. Thus, finding the shortest path for every pair of initial and goal configurations reduces to solving systems of equations for the path parameters.

As it was seen in Section VI, numerical computations show that minimum wheel-rotation cost-to-go function is similar to Reeds-Shepp cost-to-go function. Moreover, a collection of Reeds-Shepp curves are among minimum wheel-rotation trajectories. This may suggest that minimum wheel-rotation cost-to-go function is equal to Reeds-Shepp cost-to-go function. However, since loose minimum wheel-rotation trajectories are composed of rotation in place and swing segments, they are not identical with equivalent Reeds-Shepp curves. Regions of activity of different minimum wheel-rotation trajectories and the relationship between Reeds-Shepp cost and minimum wheel-rotation in general remain open questions.

References

[1] Devin J. Balkcom and Matthew T. Mason. Time optimal trajectories for bounded velocity differential drive vehicles. *Int. J. Robot. Res.*, 21(3):199–218, March 2002.

[2] H. Chitsaz, S.M. LaValle, D.J. Balkcom, and M.T. Mason. Minimum wheel-rotation paths for differential-drive mobile robots. In *IEEE Int. Conf. Robot. & Autom.*, 2006.

[3] M. Chyba and S. Sekhavat. Time optimal paths for a mobile robot with one trailer. In *IEEE/RSJ Int. Conf. on Intelligent Robots & Systems*, volume 3, pages 1669–1674, 1999.

[4] L. E. Dubins. On curves of minimal length with a constraint on average curvature, and with prescribed initial and terminal positions and tangents. *American Journal of Mathematics*, 79:497–516, 1957.

[5] L.S. Pontryagin, V.G. Boltyanskii, R.V. Gamkrelidze, and E.F. Mishchenko. *The Mathematical Theory of Optimal Processes*. John Wiley, 1962.

[6] J. A. Reeds and L. A. Shepp. Optimal paths for a car that goes both forwards and backwards. *Pacific J. Math.*, 145(2):367–393, 1990.

[7] S. Sekhavat and J.-P. Laumond. Topological property for collision-free nonholonomic motion planning: the case of sinusoidal inputs for chained form systems. *IEEE Transactions on Robotics and Automation*, 14(5):671–680, 1998.

[8] P. Souères and J.-D. Boissonnat. Optimal trajectories for nonholonomic mobile robots. In J.-P. Laumond, editor, *Robot Motion Planning and Control*, pages 93–170. Springer, 1998.

[9] P. Souères and J. P. Laumond. Shortest paths synthesis for a car-like robot. In *IEEE Transactions on Automatic Control*, pages 672–688, 1996.

[10] Héctor Sussmann. The markov-dubins problem with angular acceleration control. In *Proccedings of the 36th IEEE Conference on Decision and Control, San Diego, CA*, pages 2639–2643. IEEE Publications, 1997.

[11] Héctor Sussmann and Guoqing Tang. Shortest paths for the Reeds-Shepp car: A worked out example of the use of geometric techniques in nonlinear optimal control. Technical Report SYNCON 91-10, Dept. of Mathematics, Rutgers University, 1991.

[12] M.I. Zelikin and V.F. Borisov. *Theory of Chattering Control*. Birkhäuser, Boston, NJ, 1994.